Base of Pore Loop Is Important for Rectification, Activation, Permeation, and Block of Kir3.1/Kir3.4

S. M. Y. Makary, T. W. Claydon, K. M. Dibb, and M. R. Boyett
Division of Cardiovascular and Endocrine Sciences, University of Manchester, Manchester M13 9NT, United Kingdom

ABSTRACT The Kir3.1/Kir3.4 channel is an inward rectifier, agonist-activated K^+ channel. The location of the binding site within the channel pore that coordinates polyamines (and is thus responsible for inward rectification) and the location of the gate that opens the channel in response to agonist activation is unclear. In this study, we show, not surprisingly, that mutation of residues at the base of the selectivity filter in the pore loop and second transmembrane domain weakens Cs^+ block and decreases selectivity (as measured by Rb^+ and spermine permeation). However, unexpectedly, the mutations also weaken inward rectification and abolish agonist activation of the channel. In the wild-type channel and 34 mutant channels, there are significant ($p < 0.05$) correlations among the K_D for Cs^+ block, Rb^+ and spermine permeation, inward rectification, and agonist activation. The significance of these findings is discussed. One possible conclusion is that the selectivity filter is responsible for inward rectification and agonist activation as well as permeation and block.

INTRODUCTION

The Kir3.1/Kir3.4 channel is an inward rectifier K^+ channel in the heart. Inward rectification is caused by voltage-dependent block of the channel by intracellular Mg^{2+} and polyamines such as spermine (1). In the Kir2.1 channel, a number of residues within the pore-lining second transmembrane domain (TM2) and proximal C-terminus have been shown to be important for inward rectification (2–6). However, the regions of the channel that coordinate Mg^{2+} and polyamines within the pore are still debated. In one model, polyamines are stably coordinated within the intracellular pore by tethering the trailing end of the polyamine molecule at E-224 and E-299 in the proximal C-terminus and the leading head of the molecule at D-172 in TM2 in the internal cavity of the channel below the entrance to the selectivity filter (7,8). This model satisfies the observation that mutation of D-172 reduces the affinity of Kir2.1 by up to 40× for long bis-amines but by only 2–3 times for short bis-amines, whereas mutation of E-224 and E-299 moderately reduces the affinity for all bis-amines (7,8). In a second model, polyamines are stably coordinated within the selectivity filter (9,10). This selectivity filter model satisfies the observations that i), extracellular polyamines can permeate Kir3.1/Kir3.4 to such an extent that significant polyamine current can be measured—this shows that polyamines can interact with and pass through the selectivity filter (9,11); ii), in Kir3.1/Kir3.4, disrupting the normal structure of the selectivity filter by breaking a salt bridge behind the selectivity filter in Kir3.4 leads to a loss of inward rectification (9); and iii), in Kir6.2, introduction of negatively charged glutamate residues within the internal cavity as deep as the entrance to the selectivity filter produces strong inward rectification (glutamate residues near to the selectivity filter promote short diamine block, whereas those farther away promote longer diamine block) (10). The selectivity filter model (9,10) is supported by the observation that mutation of E-224 and E-299 in the proximal C-terminus of Kir2.1 slows the entry and exit of the polyamine spermine to and from its blocking site without eliminating the pore block component of polyamine block (although it does abolish the surface charge reduction component of polyamine block) (4,12). Modification of introduced cysteine residues below the internal cavity of the Kir6.2 channel by a positively charged (2-aminoethyl)methanethiosulfonate (MTSEA) molecule also does not affect steady-state inward rectification, only the entry and exit of spermine (10). In this study, we show that mutation of residues lining the pore at the internal entrance to the selectivity filter alters both spermine permeability and inward rectification of Kir3.1/Kir3.4 and we suggest that polyamines bind within the selectivity filter to generate inward rectification and the strength of inward rectification is in part determined by how readily polyamines can permeate the selectivity filter.

The Kir3.1/Kir3.4 channel is activated by $G_{\beta\gamma}$ subunits released on binding of an agonist to a G protein-coupled receptor. Although it has been suggested that agonist activation involves a rotation and displacement of TM2 and the opening of the ''bundle crossing'' region (an intracellular gate) (13–15), evidence suggests that an extracellular gate at the selectivity filter may exist in inward rectifier K^+ channels (16–18). For example, breaking a salt bridge behind the selectivity filter abolishes agonist activation of the Kir3.1/Kir3.4 channel (16). In this study, we show that mutation of the residues that line the pore at the internal entrance to the selectivity filter also abolishes agonist activation of the

Submitted August 30, 2005, and accepted for publication January 13, 2006.

S. M. Y. Makary and T. W. Claydon contributed equally to this work.

Address reprint requests to Professor M. R. Boyett, Division of Cardiovascular and Endocrine Sciences, University of Manchester, Core Technology Facility, 46 Grafton St. Manchester M13 9NT, UK. Tel.: +44-161-275-1192; Fax: +44-161-275-1233; E-mail: mark.boyett@manchester.ac.uk.

0006-3495/06/06/4018/17 $2.00

doi: 10.1529/biophysj.105.073569

Kir3.1/Kir3.4 channel. One possible conclusion from this finding is that the rotation and displacement of TM2 during agonist activation of the Kir3.1/Kir3.4 channel leads to a structural rearrangement and opening of the selectivity filter (an extracellular gate).

MATERIALS AND METHODS

Channel expression

Site-directed mutagenesis on Kir3.1 and Kir3.4 and preparation of cRNA was carried out as described previously (16). Oocytes were injected with cRNA encoding wild-type or mutant Kir3.1 and Kir3.4 and the human dopamine D_2 (hD_2) receptor (required for activation of the channel). Oocytes were prepared and injected with cRNA as described previously (19). cRNA (50 nl total volume) encoding wild-type or mutant Kir3.1 and Kir3.4 was injected at a concentration of 30 ng/μl, whereas cRNA encoding the hD_2 receptor was injected at a concentration of 3.8 ng/μl. After injection, oocytes were incubated at 19°C for 1–3 days in Barth's medium (in mM): 88 NaCl, 1 KCl, 2.4 $NaHCO_3$, 0.82 $MgSO_4$, 0.33 $Ca(NO_3)_2$, 0.41 $CaCl_2$, 20 HEPES, 1.25 sodium pyruvate, 0.1 mg/ml neomycin (Sigma, Poole, UK), 100 units/0.1 mg/ml penicillin/streptomycin mix (Sigma), pH 7.4 with NaOH.

Electrophysiology

Currents were recorded using the two-electrode voltage clamp technique. All oocytes were initially perfused with ND96 solution (in mM: 96 NaCl, 3 KCl, 1 $MgCl_2$, 2 $CaCl_2$, 5 HEPES, pH 7.4 with NaOH). Experimental recordings were made in a 90 mM K^+ solution (in mM: 90 KCl, 2 $CaCl_2$, 5 HEPES, pH 7.4 with KOH). To activate the hD_2 receptor, 10 μM dopamine was added to the recording solution (along with 10 μM ascorbic acid to prevent dopamine oxidation). Currents were recorded during 750-ms voltage clamp pulses from −130 to +40 or +60 mV from a holding potential of 0 mV. To measure channel block, $CsCl_2$ was added to the 90 mM K^+ recording solution at the concentrations shown. To measure permeation, the 90 mM KCl of the recording solution was substituted by 90 mM RbCl or spermine chloride. The junction potential created when using spermine chloride was measured with a flowing 3M KCl electrode with reference to ND96 solution and was +17 mV. Where important, data are corrected for junction potentials and this is stated. To measure agonist activation, currents were recorded in the absence of dopamine and then after 2 min perfusion of solution containing 10 μM dopamine. Analysis was carried out using Clampfit (Axon Instruments, Union City, CA) and SigmaPlot (SPSS Science, Chicago, IL) software. Data are presented as mean ± SE (n = number of oocytes). The comparative model of the Kir3.1/Kir3.4 tetrameric channel was constructed based on the crystal structure of KcsA as described previously (9).

RESULTS

Residues of interest at the base of the selectivity filter

Fig. 1 shows a comparative model of the Kir3.1/Kir3.4 channel based on the KcsA crystal structure (16,20). In Fig. 1 *A*, three of the four transmembrane subunits that form the functional Kir3.1/Kir3.4 heterotetramer are shown (one Kir3.4 subunit has been removed for clarity). At the base of the selectivity filter, the alanine residue at position 142 in Kir3.1 (Kir3.1-A-142) is highlighted along with the equivalent residue in Kir3.4, the threonine residue at position 148 (Kir3.4-T-148) (see Fig. 1 *C*). Also highlighted are the TM2 serine residue at position 166 in Kir3.1 (Kir3.1-S-166) and the alanine residue at the equivalent position in Kir3.4 (Kir3.4-A-172). Fig. 1 *B* shows a view from the intracellular side of the channel looking up through the channel pore. All four subunits are shown and residues Kir3.1-A-142, Kir3.4-T-148, Kir3.1-S-166, and Kir3.4-A-172 are highlighted. The model in Fig. 1, *A* and *B*, reveals that Kir3.1-A-142, Kir3.4-T-148, Kir3.1-S-166, and Kir3.4-A-172 all lie in the same horizontal plane, circling the pore at the base of the selectivity filter. Fig. 1 *C* shows a sequence alignment of a number of inward rectifier K^+ channels in which the residues at the equivalent positions are highlighted in color (*red* and *yellow*). In Kir3.1/Kir3.4 and Kir2.1, glutamate and arginine residues behind the selectivity filter have been suggested to form a salt bridge (16,21) and these residues are also highlighted in Fig. 1 *A* for Kir3.1 (Kir3.1-E-139 and Kir3.1-R-149). The glutamate and arginine residues are conserved in Kir channels as shown in Fig. 1 *C* (residues highlighted in *gray*).

Mutations at the base of the selectivity filter alter Cs^+ block and Rb^+ permeation

In the Kir2.1 channel, the equivalent residue to Kir3.1-A-142 and Kir3.4-T-148 is Kir2.1-T-141 and the equivalent residue to Kir3.1-S-166 and Kir3.4-A-172 is Kir2.1-S-165 (Fig. 1 *C*). Thompson et al. (22) showed that, in Kir2.1, mutation of either Kir2.1-T-141 to a valine residue (V) or Kir2.1-S-165 to a leucine residue (L) dramatically reduces Cs^+ block and increases Rb^+ permeation, and Thompson et al. (22) suggested that these residues contribute to a Cs^+ and Rb^+ binding site. Fig. 2 shows the effect of the equivalent mutations in the Kir3.1/Kir3.4 channel on Cs^+ block. The wild-type Kir3.1/Kir3.4 channel is given the notation **ATAT/SASA**, because it has two A-142 residues in Kir3.1 and two T-148 residues in Kir3.4 (**ATAT**) and two S-166 residues in Kir3.1 and two A-172 residues in Kir3.4 (**SASA**). In the mutant VVVV/**SASA** channel (bold type used for wild-type sequence), Kir3.1-A-142 and Kir3.4-T-148 were both replaced with a valine residue. In the mutant **ATAT**/LLLL channel, Kir3.1-S-166 and Kir3.4-A-172 were both replaced with a leucine residue. Fig. 2 *A* shows typical current traces recorded from wild-type and mutant channels during 750-ms voltage clamp pulses from −130 to +40 mV from a holding potential of 0 mV in the absence and presence of 10 mM extracellular Cs^+. Cs^+ blocked the wild-type (**ATAT/SASA**) channel. This is also shown by the mean current-voltage relationships recorded in the presence of various concentrations of Cs^+ in Fig. 2 *B*. From these data, dose-response curves were plotted (Fig. 2 *C*). The dissociation constant, K_D, at −130 mV was 178 ± 4 μM ($n = 6$), which is comparable with that of 101 ± 7 μM (at −97 mV) reported for Kir2.1 (22). In both the mutant VVVV/**SASA** and the **ATAT**/LLLL channels, Cs^+ block was reduced ~8-fold

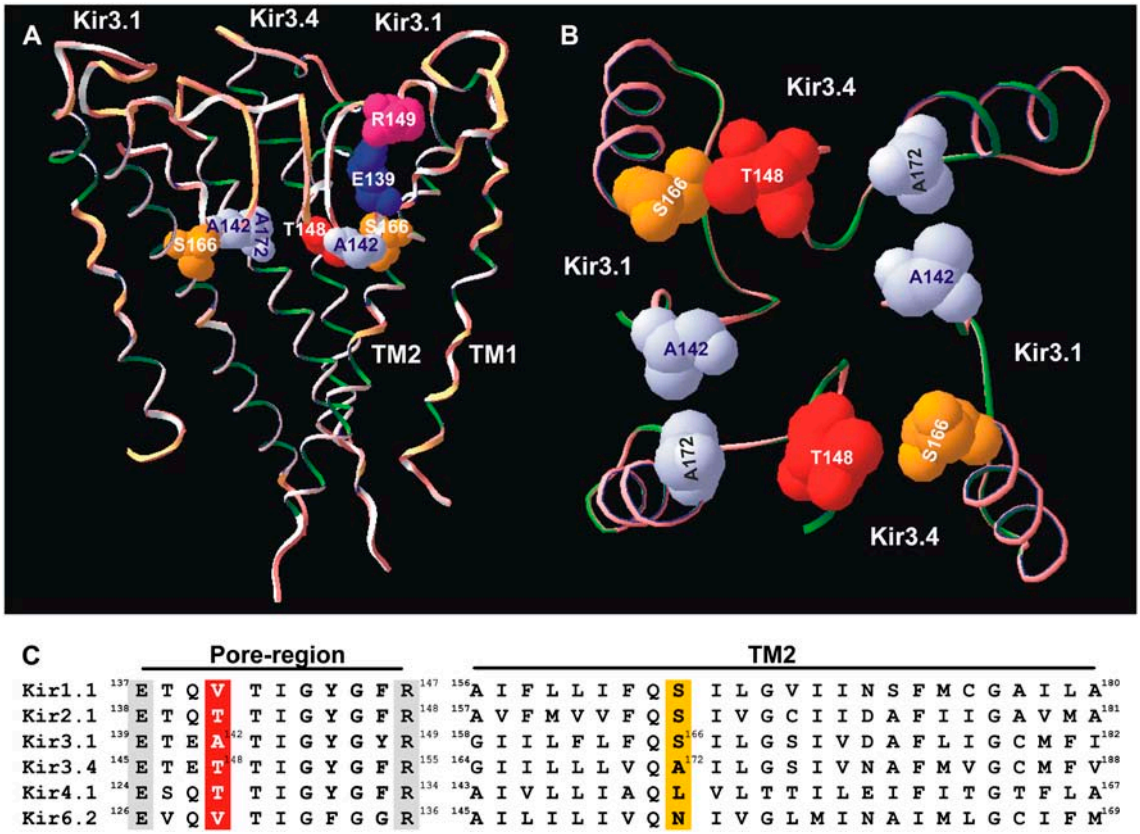

FIGURE 1 Model of the Kir3.1/Kir3.4 channel. (*A*) Model of the TM1-P-TM2 domains of the Kir3.1/Kir3.4 tetramer based on the KcsA crystal structure. The residues of interest are highlighted as space-filled models. Only three of the four subunits are shown for clarity (one Kir3.4 subunit has been removed). (*B*) An enlarged cross-sectional view looking up at the base of the selectivity filter. (*C*) An alignment of the pore region (*left*) and TM2 domains (*right*) in a number of inward rectifier K^+ channels. Residues of interest are highlighted.

(Fig. 2, *A* and *B*); the K_D at −130 mV was increased to 1545 ± 384 and 2873 ± 583 μM, respectively (Fig. 2 *C*; $n = 5$; ANOVA, $p < 0.05$). This reduction in Cs^+ sensitivity is, however, conservative in comparison with the ~40- and 180-fold reductions caused by the T-141V (VVVV) and S-165L (LLLL) mutations, respectively, in Kir2.1 (22). Fig. 2 *D* shows how the K_D of Cs^+ block of the Kir3.1/Kir3.4 channel varied with voltage. From this, δ, the apparent fraction of the electrical field that Cs^+ must cross to reach its blocking site, was calculated (over the potential range −130 to −50 mV). δ was 0.99 in the wild-type (**ATAT/SASA**) channel and 2.2 and 1.8, respectively, in the mutant VVVV/**SASA** and **ATAT**/LLLL channels; the mutations may have altered the site of Cs^+ block or increased the number of K^+ ions needed to be moved (as a result of an increase in K^+ occupancy) for block to occur (even if block occurred at the same site). To study Rb^+ permeation, the 90 mM KCl in the bathing solution was replaced by 90 mM RbCl (Fig. 3). Rb^+ permeated the wild-type (**ATAT/SASA**) channel to a certain extent; at −130 mV, in this series of experiments, the Rb^+ current was 0.3 ± 0.02 the size of the K^+ current ($n = 5$; Fig. 3 *A*). Rb^+ permeation was significantly increased in the mutant VVVV/**SASA** and **ATAT**/LLLL channels and the Rb^+ current was 0.57 ± 0.06 ($n = 7$) and 0.73 ± 0.01 ($n = 5$), respectively, the size of the K^+ current (Fig. 3, *B* and *C*; ANOVA, $p < 0.01$ compared with the wild-type channel). This increase in Rb^+ permeation is conservative, however, compared with the ~3- and 15-fold increases caused by the T-141V (VVVV) and S-165L (LLLL) mutations, respectively, in Kir2.1 (22).

Mutations at the base of the selectivity filter alter spermine permeation and inward rectification

Previously, we have demonstrated spermine permeation of Kir3.1/Kir3.4 by replacing the 90 mM KCl in the bathing solution by 90 mM spermine chloride (9,11). Spermine permeation of the wild-type (**ATAT/SASA**) channel can be seen in the typical current traces and mean current-voltage relationships in Fig. 4 *B*. There was substantial inward current, which was absent in uninjected oocytes (Fig. 4 *A*), through the wild-type (**ATAT/SASA**) channel in the presence of 90 mM extracellular spermine (Fig. 4 *B*). The spermine current through the wild-type (**ATAT/SASA**) channel at −130 mV was 0.36 ± 0.04 ($n = 5$) the size of

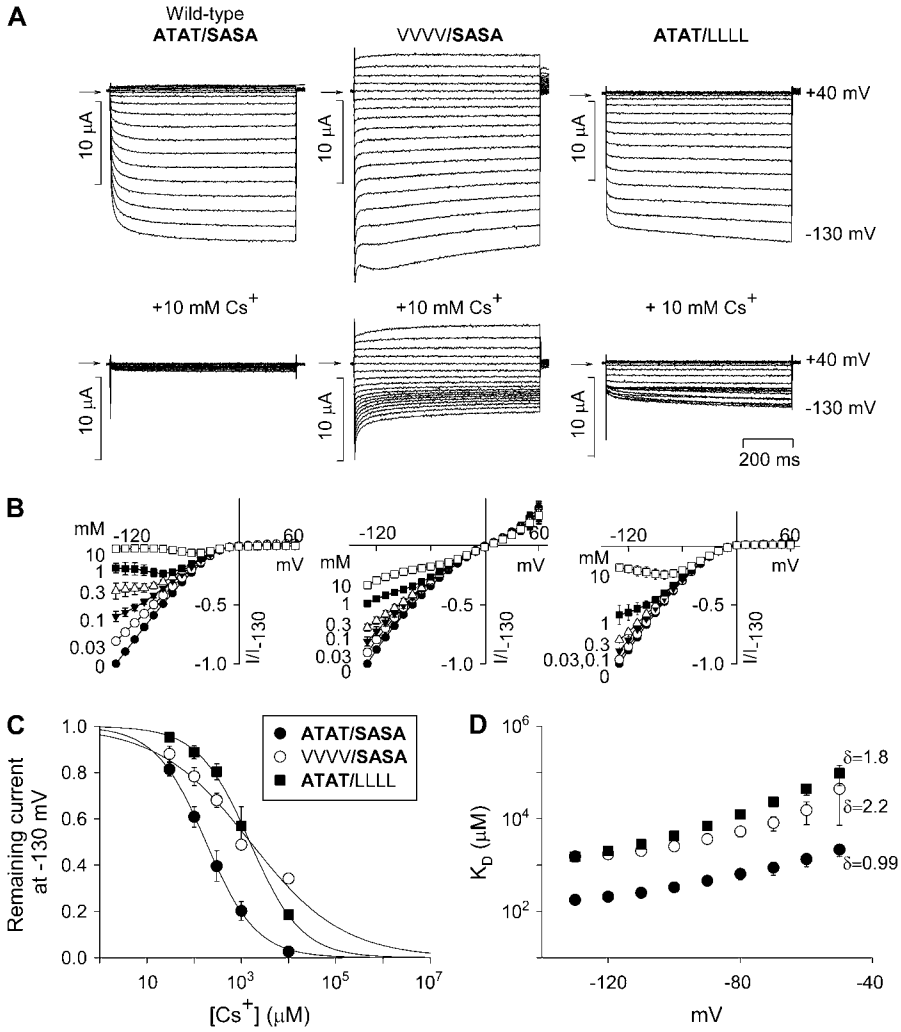

FIGURE 2 Mutations at the base of the selectivity filter alter Cs^+ block. (*A*) Typical current traces recorded during voltage pulses from −130 to +40 mV from wild-type (**ATAT/SASA**) and Kir3.1-A-142V/Kir3.4-T-148V (VVVV/**SASA**) and Kir3.1-S-166L/Kir3.4-A-172L (**ATAT/**LLLL) mutant channels. Currents were recorded in the absence (*top*) and presence (*bottom*) of 10 mM Cs^+. Arrows indicate zero current. (*B*) Mean normalized current-voltage relationships for each channel in the presence of a range of Cs^+ concentrations. (*C*) Dose-response curves for Cs^+ block at −130 mV of each channel (indicated in *inset*). (*D*) Mean K_D for Cs^+ block versus membrane potential for each channel (indicated in *inset* in *C*). The value of δ, the apparent fraction of the electrical field that Cs^+ must cross to reach its blocking site, for each channel is shown. Mean ± SE shown ($n = 5$–6).

the current carried by K^+ (Fig. 4 *B*). Just as Rb^+ permeation was increased in the mutant VVVV/**SASA** channel, spermine permeation was also greatly increased (Fig. 4 *C*). Spermine current through the mutant channel was 0.76 ± 0.2 the size of the K^+ current (Fig. 4 *C*; $n = 9$; ANOVA, $p <$ 0.001 compared with the wild-type channel). In contrast, spermine permeation was decreased in the mutant **ATAT/**LLLL channel (Fig. 4 *D*). Spermine current through the mutant channel was 0.17 ± 0.02 the size of the K^+ current (Fig. 4 *D*; $n = 5$; ANOVA, $p = 0.005$ compared with the wild-type channel). We have suggested previously that the degree to which polyamines can permeate inward rectifier K^+ channels may determine the strength of inward rectification (11). The rationale behind this is that inward rectification will be weaker if polyamines permeate rather than block the channel. Consistent with this, Fig. 4, *C* and *D*, shows that inward rectification was weakened in the mutant VVVV/**SASA** channel, but not in the mutant **ATAT/**LLLL channel. The ratio of the conductance at +40 mV to that at −100 mV ($g_{+40\ mV}/g_{-100\ mV}$), a measure of the strength of inward rectification, was 0.06 ± 0.007 ($n = 15$) in the wild-type (**ATAT/SASA**) channel. This was increased, i.e., inward rectification was weakened, in the mutant VVVV/**SASA** channel to 0.7 ± 0.09 ($n = 6$; ANOVA, $p = 0.005$ compared with the wild-type channel), whereas in the mutant **ATAT/**LLLL channel it remained low (0.07 ± 0.02; $n = 5$; ANOVA, not significantly different from the wild-type channel).

Relative importance of Kir3.1 and Kir3.4 at the base of the selectivity filter

Because the Kir3.1/Kir3.4 channel is a heterotetramer, it is asymmetric and various studies have shown that equivalent residues in Kir3.1 and Kir3.4 do not necessarily play the same roles qualitatively and/or quantitatively (23,24). We investigated the effect of mutations at the internal entrance to the selectivity filter further, and Fig. 5 compares the contributions of the Kir3.1 and Kir3.4 subunits to the changes in Cs^+ block, Rb^+ permeation, spermine permeation, and the

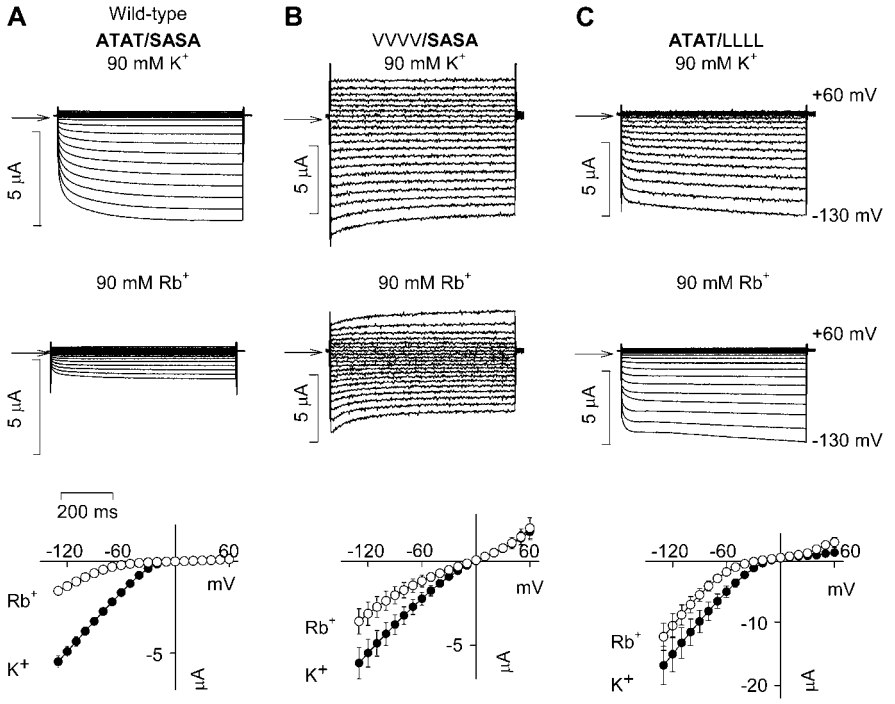

FIGURE 3 Mutations at the base of the selectivity filter alter Rb^+ permeation. (*Top*) Typical current traces recorded during voltage pulses from −130 to +60 mV from wild-type (**ATAT/SASA**) and Kir3.1-A-142V/Kir3.4-T-148V (VVVV/**SASA**) and Kir3.1-S-166L/Kir3.4-A-172L (**ATAT/**LLLL) mutant channels with K^+ or Rb^+ as the charge carrier. Currents were recorded in 90 mM extracellular K^+ or 90 mM extracellular Rb^+. Arrows indicate zero current. (*Bottom*) Mean normalized current-voltage relationships for each channel with K^+ or Rb^+ as the charge carrier. Mean ± SE shown ($n = 5$–9).

strength of inward rectification (K_D for Cs^+ block at −130 mV, Rb^+ current at −130 mV, spermine current at −130 mV, and $g_{+40\ mV}/g_{-100\ mV}$ shown). Fig. 5 *A* shows the effects when Kir3.1-A-142 and/or Kir3.4-T-148 were replaced by valine residues, and Fig. 5 *B* shows the effects when Kir3.1-S-166 and/or Kir3.4-A-172 were replaced by leucine residues. In every case, the mutation in Kir3.4 alone (AVAV and SLSL) had qualitatively the same effect as the

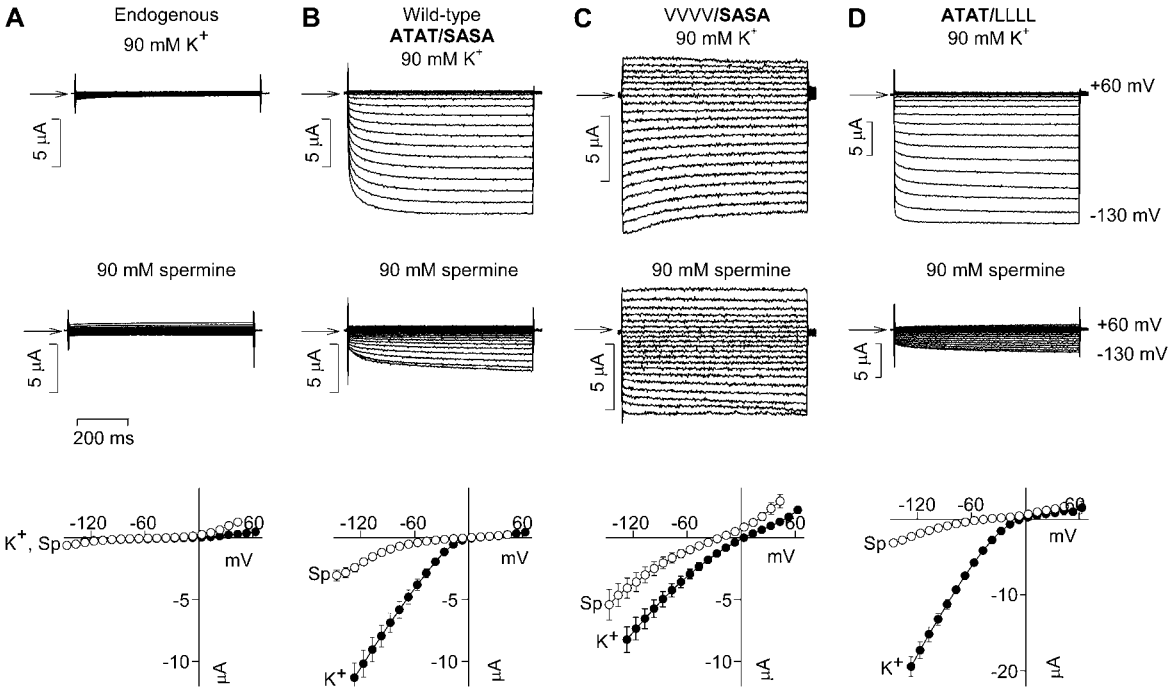

FIGURE 4 Mutations at the base of the selectivity filter alter spermine permeation. (*Top*) Typical current traces recorded during voltage pulses from −130 to +60 mV from endogenous, wild-type (**ATAT/SASA**), Kir3.1-A-142V/Kir3.4-T-148V (VVVV/**SASA**) and Kir3.1-S-166L/Kir3.4-A-172L (**ATAT/**LLLL) channels with K^+ or spermine as the charge carrier. Currents were recorded in 90 mM extracellular K^+ or 90 mM extracellular spermine. Arrows indicate zero current. (*Bottom*) Mean normalized current-voltage relationships for each channel with K^+ or spermine as the charge carrier. Mean ± SE shown ($n = 5$–9). Data corrected for junction potentials.

double mutations in both Kir3.1 and Kir3.4 (VVVV and LLLL), whereas the mutation in Kir3.1 alone (VTVT and LALA) did not (Fig. 5). The effects of mutations in Kir3.1 alone could be qualitatively different from the effects of mutations in both subunits (spermine current—VTVT versus VVVV; Cs^+ block—LALA versus LLLL). In some cases, the effect of the mutation in Kir3.4 alone was quantitatively the same as the effect of the double mutations in both Kir3.1 and Kir3.4 (compare Cs^+ block and Rb^+ permeation of the SLSL and LLLL mutant channels). These data suggest that the residues in Kir3.4 play a more important role in block and permeation than those in Kir3.1.

Effect of the size and polarity of the residues at the base of the selectivity filter at the Kir3.1-A-142/ Kir3.4-T-148 position

The alanine residue (at position 142 in wild-type Kir3.1) is a small nonpolar residue, whereas the threonine residue (at position 148 in wild-type Kir3.4) is a large polar residue

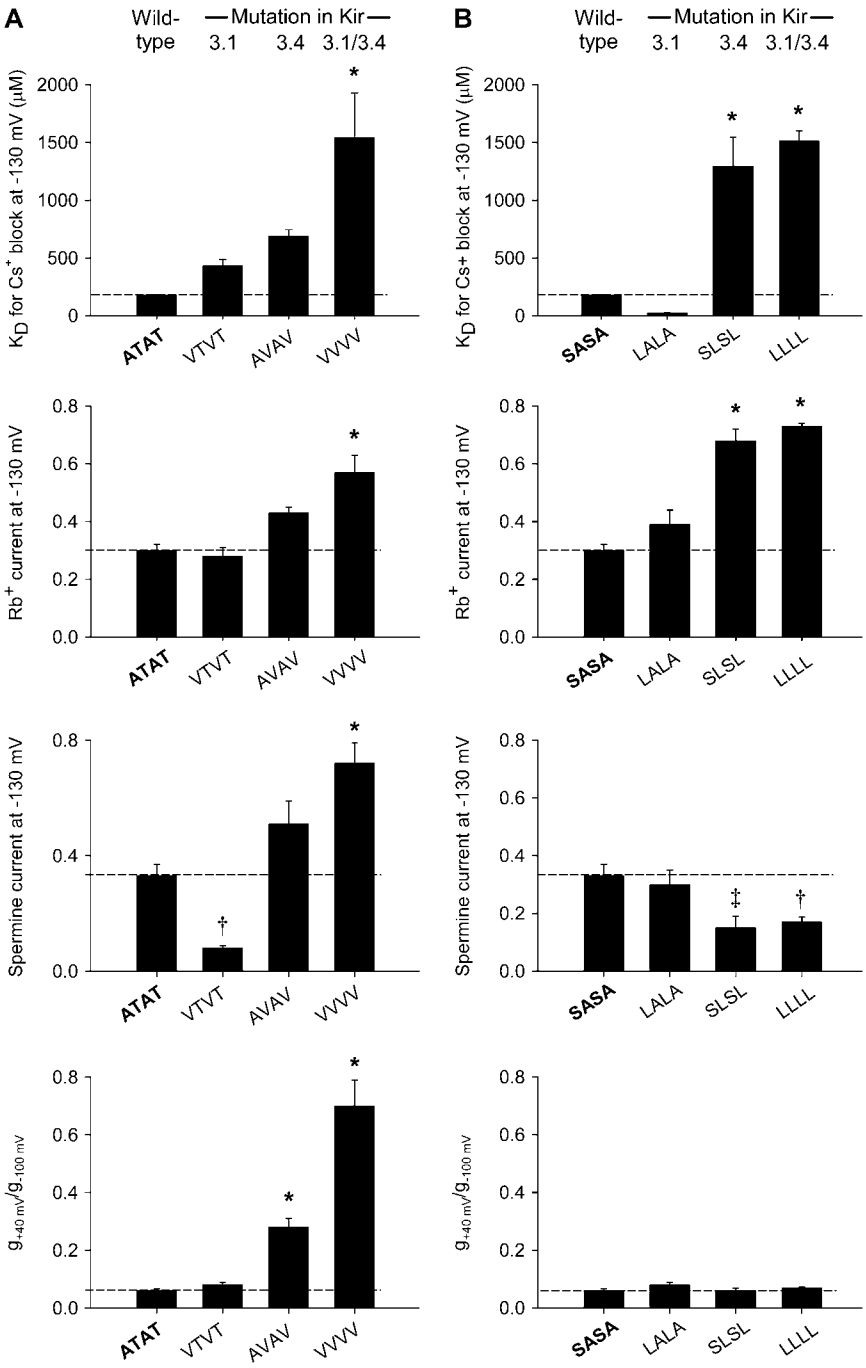

FIGURE 5 Summary of the effects of mutations at the base of the selectivity filter on block, permeation, and inward rectification. (*A* and *B*) Summary of the effects of different combinations of mutations of Kir3.1-A-142 and/or Kir3.4-T-148 (*A*) and Kir3.1-S-166 and/or Kir3.4-A-172 (*B*) on the K_D (at −130 mV) of Cs^+ block, Rb^+ current (at −130 mV), spermine current (at −130 mV), and inward rectification ($g_{+40\ mV}/g_{-100\ mV}$). Mean ± SE shown ($n = 5$–15). $^*p < 0.001$, $^‡p < 0.01$, and $^†p < 0.05$ as compared to the wild-type channel (one-way ANOVA). Data corrected for junction potentials.

and in the experiments above we replaced them both by a valine residue, a large nonpolar residue. To investigate whether the size and polarity of the residue introduced is important, in Fig. 6 *A* we compare the effects of replacing Kir3.1-A-142 and Kir3.4-T-148 in the wild-type channel (**ATAT**; two small nonpolar residues and two large polar residues) by threonine residues (resulting in TTTT, four large polar residues), alanine residues (resulting in AAAA, four small nonpolar residues), or valine residues (resulting in VVVV, four large nonpolar residues). In the case of Cs^+ block and inward rectification, the size and polarity of the introduced residue appears to be important, because marked changes were observed only when four large nonpolar valine residues were introduced, but not when four large polar threonine or four small nonpolar alanine residues were introduced (Fig. 6 *A*). In the case of Rb^+ permeation (and perhaps spermine permeation), the polarity alone appears to be important, because marked changes were observed when either four small nonpolar alanine or four large nonpolar valine residues were introduced but not

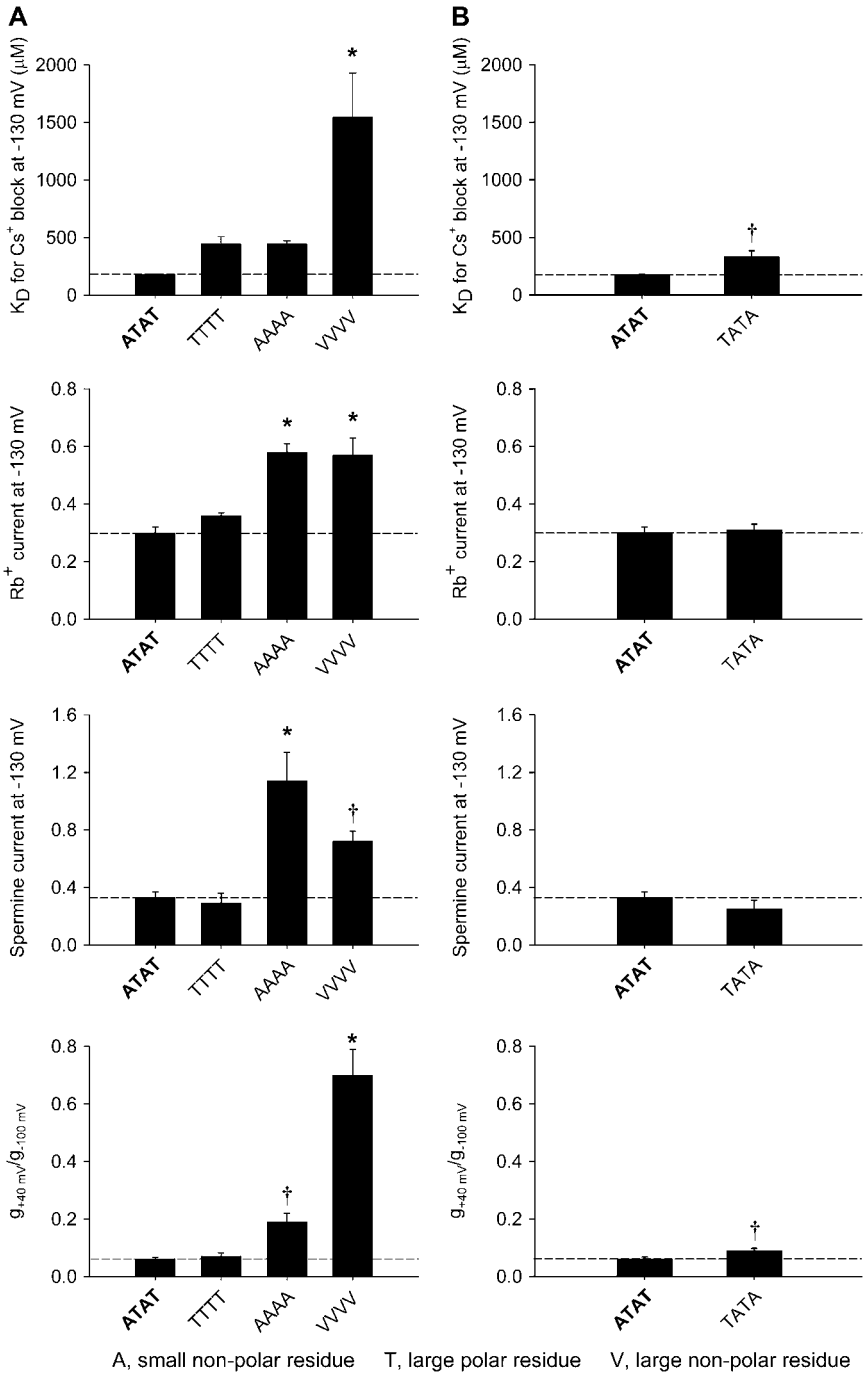

FIGURE 6 Summary of the effects of the size and charge of the residue at position Kir3.1-A-142/Kir3.4-T-148 on block, permeation, and inward rectification. (*A* and *B*) Summary of the effects of the size and charge of the residue at position Kir3.1-A-142/Kir3.4-T-148 (*A*) and the effect of swapping the alanine and threonine residues at position Kir3.1-A-142/Kir3.4-T-148 (*B*) on the K_D (at −130 mV) of Cs^+ block, Rb^+ current (at −130 mV), spermine current (at −130 mV), and inward rectification ($g_{+40\ mV}/g_{-100\ mV}$). Mean ± SE shown (n = 5–15). *$p < 0.001$ and $^{\dagger}p < 0.05$ as compared to the wild-type channel (one-way ANOVA). Data corrected for junction potentials.

when four large polar threonine residues were introduced (Fig. 6 *A*).

Fig. 6 *B* shows that swapping the small nonpolar alanine and large polar threonine residues between Kir3.1 and Kir3.4 had no substantial effect on any of the measured channel properties.

Interactions at the base of the selectivity filter

We next investigated whether the residues in the pore loop (Kir3.1-A-142 and Kir3.4-T-148) might interact with those in TM2 (Kir3.1-S-166 and Kir3.4-A-172). Fig. 7 shows the effect of combinations of mutations at both sites on Cs^+ block and Rb^+ permeation. For this series of experiments, for convenience, we chose to mutate Kir3.4-T-148 to an alanine residue (AAAA in Fig. 7) and Kir3.1-S-166 and Kir3.4-A-172 to leucine residues (LLLL in Fig. 7). Fig. 7 *A* shows that the effect of the combined mutations (AAAA/LLLL) on Cs^+ block was much greater than the effects of the individual mutations. This result suggests that Kir3.1-A-142/Kir3.4-T-148 and Kir3.1-S-166/Kir3.4-A-172 (or their effects on Cs^+ block at least) interact, because the effects of the combined mutations are not simply the sum of the effects of the individual mutations. This was confirmed by the calculation of the coupling coefficient, Ω. The use of coupling coefficients was first introduced into ion channel studies by Hidalgo and MacKinnon (25). If two residues do not interact, $\Omega = 1$. In this case, $\Omega \approx 15$ (corresponding to a coupling energy of $\sim$7 kJ.mol^{-1}). Fig. 7 *B* shows that the effect of the combined mutations on Rb^+ permeation was also greater than the effects of the individual mutations.

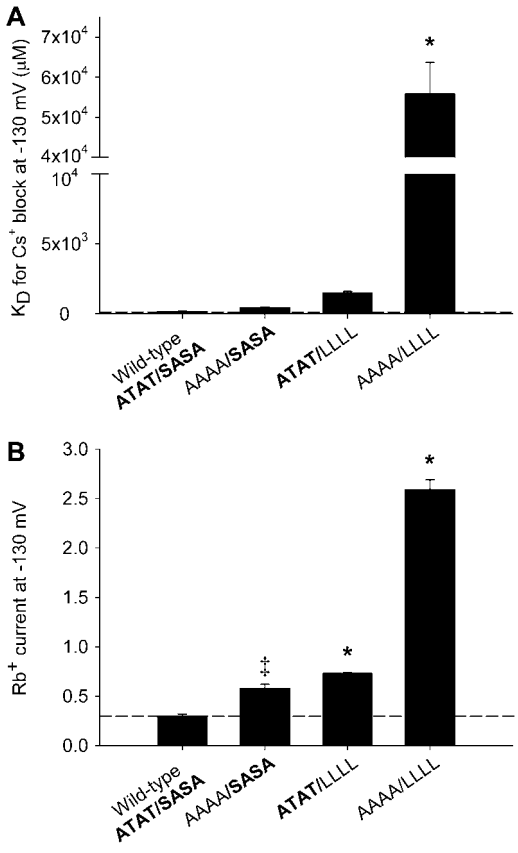

FIGURE 7 Interactions between Kir3.1-A-142/Kir3.4-T-148 and Kir3.1-S-166/Kir3.4-A-172 at the base of the selectivity filter. *A*, *B*, summary of the effects of combinations of mutations made at positions Kir3.1-A-142/Kir3.4-T-148 and Kir3.1-S-166/Kir3.4-A-172 on the K_D (at -130 mV) of Cs^+ block (*A*) and Rb^+ current (at -130 mV; *B*). Means $\pm$ SE shown ($n = 5$–6). $^*p < 0.001$ and $^‡p < 0.002$ as compared to the wild-type channel (one-way ANOVA).

Interactions with the salt bridge behind the selectivity filter

We have previously shown that disruption of the salt bridge behind the selectivity filter in Kir3.4, between Kir3.4-E-145 and Kir3.4-R-155 (Fig. 1 *C*), alters block, permeation, inward rectification, and agonist activation of the channel; the effects were attributed to an increase in the flexibility of the selectivity filter (9,16). Interestingly, mutation of the equivalent salt bridge in Kir3.1, between Kir3.1-E-139 and Kir3.1-R-149 (Fig. 1, *A* and *C*), has minimal effects on channel properties (9). The effects of the disruption of the salt bridge in Kir3.4 are similar to the effects (observed in this study) of mutation of the residues of interest at the base of the selectivity filter. Because of this, we investigated whether the salt bridge residues may interact with the residues at the base of the selectivity filter (Figs. 8 and 9). In particular, we tested the possibility that the lack of effect of disruption of the salt bridge in Kir3.1 may be linked to the asymmetry in the residues at the base of the selectivity filter.

Fig. 8 shows typical currents recorded from wild-type or mutant channels during pulses from -130 to $+40$ mV. Below are mean current-voltage relationships over a more restricted range of potentials (-60 to $+40$ mV) to highlight the extent of inward rectification in each channel. Disruption of the salt bridge in Kir3.1, by the mutation Kir3.1-E-139Q, had no effect on inward rectification (Fig. 8 *B*) as shown previously (9). Similarly, mutation of Kir3.4-T-148 to an alanine residue (Kir3.4-T-148A; resulting in a AAAA**/SASA** channel) had only a small effect on inward rectification (Fig. 8 *C*) as expected (Fig. 6 *A*). However, the double mutation (Kir3.1-E-139Q/Kir3.4-T-148A) dramatically reduced inward rectification (Fig. 8 *D*). These data are summarized in Fig. 9 *B*, which shows $g_{+40\ \mathrm{mV}}/g_{-100\ \mathrm{mV}}$, a measure of inward rectification, for each channel. Fig. 9 *A* shows that spermine permeation was also significantly and substantially increased by the double, but not by the single, mutations. Similar results were observed when Kir3.1-E-139 was mutated along with replacement of Kir3.1-A-142 with a threonine residue (the latter resulting in a TTTT**/SASA** channel), although in this case the changes in spermine permeation and inward rectification with the double mutation were less dramatic (Fig. 9, *C* and *D*). In contrast, by itself,

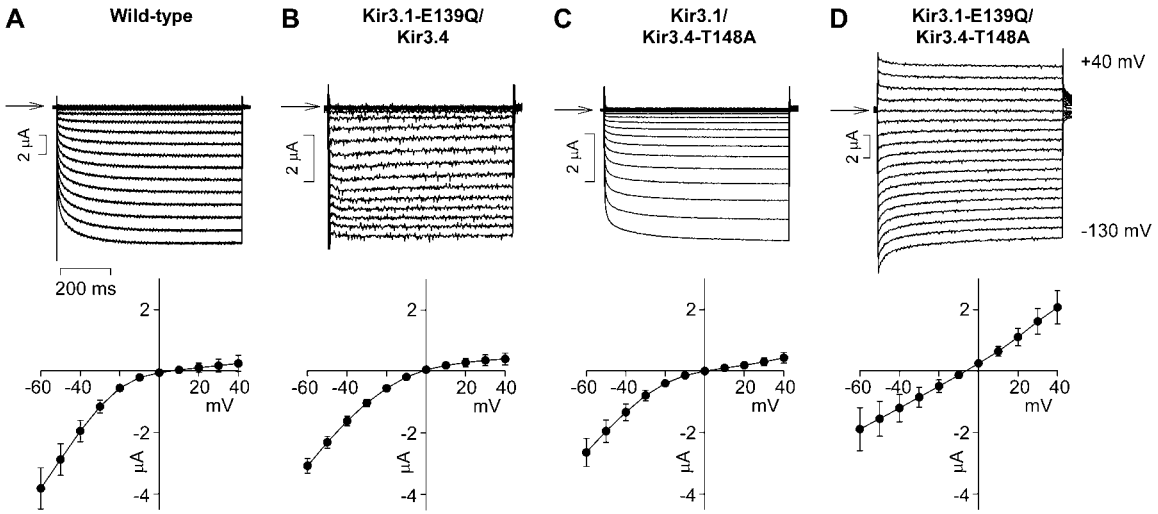

FIGURE 8 Disruption of the salt bridge behind the selectivity filter in the Kir3.1 subunit alters inward rectification when Kir3.4-T-148 is mutated. (*Top*) Typical current traces recorded during voltage pulses from −130 to +40 mV from the wild-type channel and channels in which either or both the mutations Kir3.1-E-139Q and Kir3.4-T-148A were made. Arrows indicate zero current. (*Bottom*) Mean normalized current-voltage relationships over a restricted range of potentials (−60 to +40 mV) to highlight changes in inward rectification. Mean ± SE shown ($n = 6$–7).

disruption of the salt bridge in Kir3.4, by the mutation Kir3.4-E-145Q, significantly and substantially increased spermine permeation and significantly and substantially decreased inward rectification (Fig. 9, *E* and *F*) as shown previously (9). When the salt bridge in Kir3.4 was disrupted at the same time that Kir3.4-T-148 was mutated to an alanine residue (Kir3.4-T-148A; resulting in a AAAA**/SASA** channel), the effects on spermine permeation and inward rectification were greater (Fig. 9, *E* and *F*), but the amplification was not dramatic as in the case of disruption of the salt bridge in Kir3.1 (Fig. 9, *A* and *B*).

In summary, these results suggest that the salt bridge residues in Kir3.1 and the residues at the base of the selectivity filter (or their effects at least) do interact. Furthermore, they suggest that the lack of effect of disruption of the salt bridge behind the selectivity filter in Kir3.1 is related to the residues at the base of selectivity filter: when the residues at the base of the selectivity filter are altered, breaking the salt bridge in Kir3.1 affects channel properties. Breaking the salt bridge in Kir3.4, in contrast, affects channel properties regardless of the residues at the base of the selectivity filter.

Fig. 9 shows that mutations that altered spermine permeation also altered inward rectification, strengthening the conclusion that the extent of spermine permeation determines the extent of inward rectification.

Mutations at the base of the selectivity filter also alter agonist activation

Evidence suggests that K^+ channel opening may involve a gate at the selectivity filter (16–18,26,27). Fig. 10 provides evidence for the involvement of the selectivity filter during agonist activation of the Kir3.1/Kir3.4 channel. Fig. 10 *A* shows typical currents through the wild-type (**ATAT/SASA**) and mutant VVVV/**SASA** and **ATAT**/LLLL channels in the absence (Fig. 10 *A*, *top*) and presence (Fig. 10 *A*, *middle*) of agonist (10 μM dopamine). From these traces, the agonist-activated current was obtained (Fig. 10 *A*, *bottom*). Some basal activation of the wild-type (**ATAT/SASA**) channel existed—basal current is thought to be the result of a high level of free $G_{\beta\gamma}$ and/or a low level of $G_{\alpha i}$ within the *Xenopus* oocyte (28). Nevertheless, upon application of agonist, current was increased by 51% ± 5% ($n = 6$). This is seen more clearly in the mean current-voltage relationships in Fig. 10 *B*. Just as replacement of Kir3.1-A-142 and Kir3.4-T-148 with valine residues (VVVV/**SASA**) or of Kir3.1-S-166 and Kir3.4-A-172 with leucine residues (**ATAT**/LLLL) dramatically altered Cs^+ block and Rb^+ permeation (Fig. 5), agonist activation was also dramatically altered: the mutant VVVV/**SASA** and **ATAT**/LLLL channels were no longer sensitive to agonist activation (on addition of agonist, there was no increase in current, Fig. 10). Because these mutations altered Cs^+ and Rb^+ coordination within the selectivity filter (Fig. 5) as well as agonist activation of the channel (Fig. 10), these data possibly suggest a role for the selectivity filter during agonist activation (see Discussion).

Agonist activation affects selectivity

If the selectivity filter is altered during agonist activation, it is possible that selectivity is altered. Fig. 11 *A* shows typical current traces recorded from the wild-type channel in the absence and presence of agonist (10 μM dopamine) with

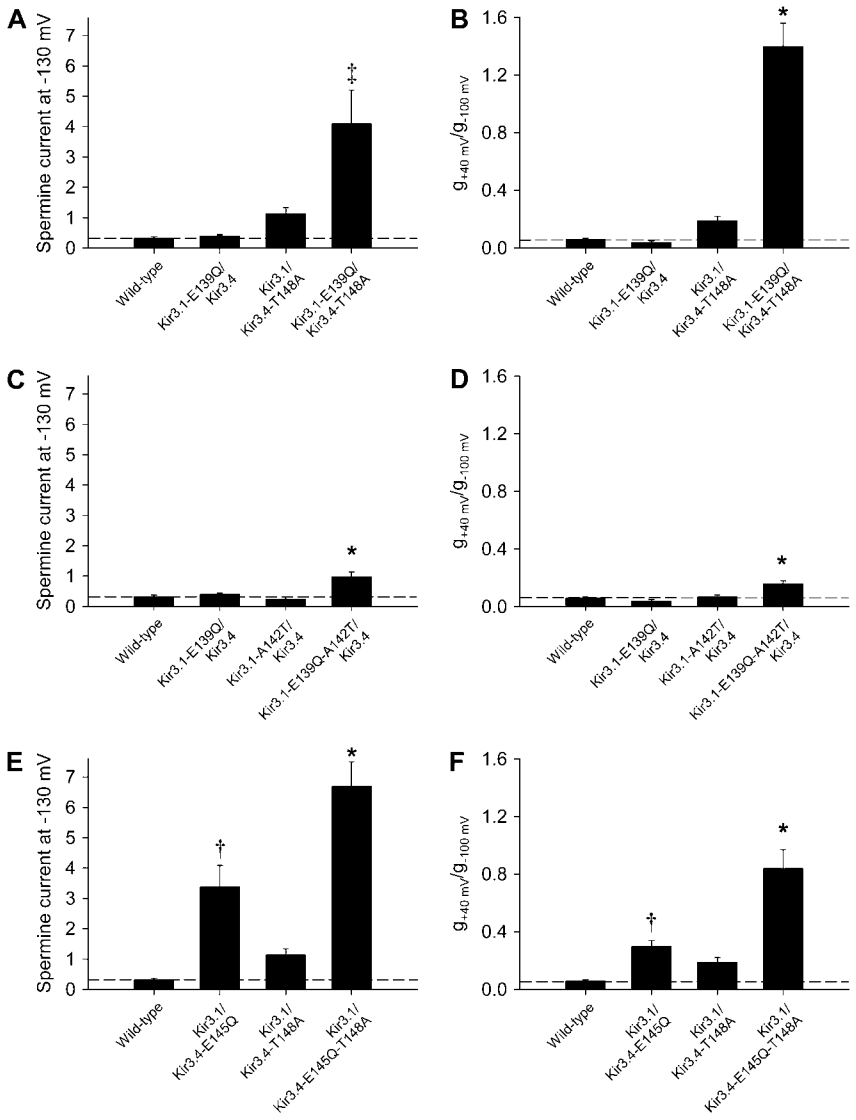

FIGURE 9 Kir3.1-A-142 and Kir3.4-T-148 interact with the salt bridge behind the selectivity filter in the Kir3.1 subunit. (*A–F*) Summary of the effects of mutation of either or both Kir3.1-E-139 and Kir3.4-T-148 (*A* and *B*), either or both Kir3.1-E-139 and Kir3.1-A-142 (*C* and *D*) and either or both Kir3.4-E-145 and Kir3.4-T-148 (*E* and *F*) on spermine current (at −130 mV) and inward rectification ($g_{+40\ mV}/g_{-100\ mV}$). Mean ± SE shown (n = 5–15). *$p <$ 0.001, $^{\ddagger}p < 0.01$, and $^{\dagger}p < 0.05$ as compared to the wild-type channel (one-way ANOVA). Data corrected for junction potentials.

90 mM K^+ or Rb^+ as the charge carrier. Currents obtained at the end of the experiment after the application of 1 mM Ba^{2+} to block Kir3.1/Kir3.4 current are also shown (Fig. 11 *A*, *bottom*); the currents are comparable to endogenous currents recorded from uninjected oocytes under the same conditions (Fig. 11 *B*). Once again, in the absence of agonist (and Ba^{2+}), there was some basal activation of Kir3.1/Kir3.4 (the current is substantially greater than the current remaining in Ba^{2+} or in uninjected oocytes), but upon application of agonist, current was increased. The current carried by Rb^+ (as a fraction of the current carried by K^+) was greatly reduced in the presence of agonist. This is confirmed by Fig. 4 *C*, which shows mean-current voltage relationships for the Ba^{2+}-sensitive current in the presence and absence of agonist with K^+ and Rb^+ as the charge carrier. At −130 mV, the Ba^{2+}-sensitive Rb^+ current was 1.59 ± 0.48 and 0.48 ± 0.02 ($n = 7$), respectively, the size of the Ba^{2+}-sensitive K^+ current in the absence and presence of agonist (Fig. 11 *B*; paired *t*-test, $p < 0.05$). It is concluded that selectivity is altered during agonist activation.

Relation among Cs^+ block, Rb^+ and spermine permeation, inward rectification, and agonist activation

During the course of this study we investigated the wild-type Kir3.1/Kir3.4 channel and 20 mutant Kir3.1/Kir3.4 channels. In previous studies (9,16) we investigated a further 14 mutant Kir3.1/Kir3.4 channels: arginine (Kir3.1-R-149, Kir3.4-R-155) and glutamate (Kir3.1-E-141, Kir3.4-E-145, Kir3.4-E-147) residues behind the selectivity filter, phenylalanine residues (Kir3.1-F-181, Kir3.4-F-187) at the bundle crossing, serine residues (Kir3.1-S-170, Kir3.4-S-176) in TM2 implicated in agonist activation, an aspartate residue (Kir3.1-D-173)

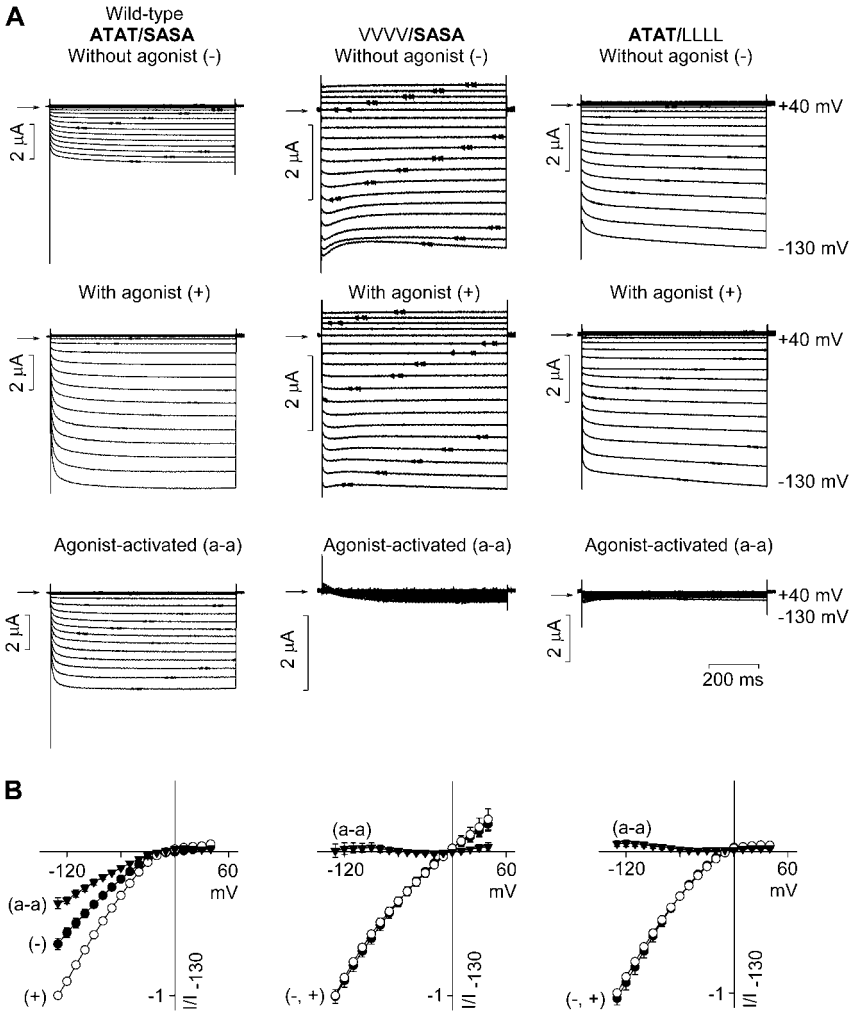

FIGURE 10 Mutations at the base of the selectivity filter abolish agonist activation. (*A*) Typical current traces recorded during voltage pulses from −130 to +40 mV from wild-type (**ATAT/SASA**) and mutant (VVVV/**SASA**) and (**ATAT**/LLLL) channels in the absence and presence of 10 μM dopamine. Agonist-activated currents (obtained by subtracting currents in the absence and presence of agonist) are also shown. (*B*) Mean normalized current-voltage relationships of each channel in the absence (−) and presence (+) of agonist and the agonist-activated (a-a) current. Mean ± SE shown ($n = 7$).

in TM2 implicated in polyamine binding, and a glutamate residue (Kir3.4-E-231) in the proximal C-terminus also implicated in polyamine binding were mutated. For all 35 channels, Fig. 12 shows that there are significant ($p < 0.05$) correlations among Cs^+ block, Rb^+ and spermine permeation, inward rectification, and agonist activation.

Fig. 12 *A* shows that a significant correlation ($p < 0.01$, $R^2 = 0.66$) exists between inward rectification and spermine permeation. This is consistent with the hypothesis that the degree to which polyamines can permeate inward rectifier K^+ channels determines the strength of inward rectification (29,30). However, there is scatter in the relationship in Fig. 12 *A* and this suggests that other factors are also involved—this is highlighted by the differing changes in spermine permeation and inward rectification with the AAAA and VVVV mutant channels (Fig. 6 *A*). There is also a significant correlation ($p < 0.05$, $R^2 = 0.52$) between inward rectification and Rb^+ permeation (Fig. 12 *B*). Fig. 12, *C* and *D*, shows that a significant correlation ($p < 0.05$, $R^2 = 0.69$; $p < 0.05$, $R^2 = 0.71$) also exists between inward rectification and Cs^+ block and agonist activation. Fig. 12, *E–G*, shows a significant correlation between agonist activation and spermine permeation, Rb^+ permeation, and Cs^+ block. One possible conclusion from these data is that both inward rectification and agonist activation are determined by the same part of the channel (i.e., the selectivity filter—but see Discussion).

DISCUSSION

In this study, we have investigated the role of residues at the base of the selectivity filter of the Kir3.1/Kir3.4 channel. These residues surround the internal entrance of the selectivity filter (Fig. 1). The results show that mutations at this point influence block, permeation, inward rectification, and agonist activation.

The residues at the internal entrance of the selectivity filter—asymmetry of the pore and interactions with other residues

Thompson et al. (22) showed that mutation of T-141 in the pore loop and S-165 in TM2 in Kir2.1 alters both Cs^+ block

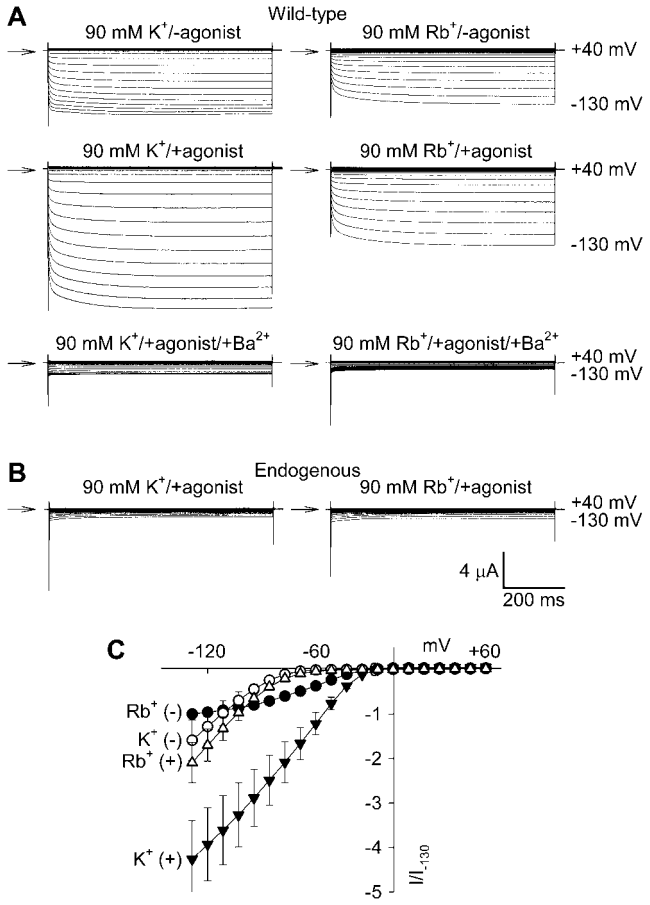

FIGURE 11 Change in selectivity during agonist activation. (*A*) Typical current traces from the wild-type channel with K^+ (*left*) or Rb^+ (*right*) as the charge carrier in the absence of dopamine (*top*), in the presence of 10 μM dopamine (*middle*), and after the subsequent addition of 1 mM Ba^{2+} (*bottom*). (*B*) Typical current traces recorded from an uninjected oocyte with K^+ (*left*) or Rb^+ (*right*) as the charge carrier in the presence of 10 μM dopamine. In *A* and *B*, currents were recorded during voltage pulses from −130 to +40 mV and arrows indicate zero current. (*C*) Mean normalized current-voltage relationships with K^+ or Rb^+ as the charge carrier and with (+) and without (−) dopamine. Mean ± SE shown ($n = 7$). Ba^{2+}-sensitive currents shown.

and Rb^+ permeation. In this study, we showed that mutations at the equivalent positions in Kir3.1/Kir3.4 also affected Cs^+ block and Rb^+ permeation (Figs. 2, 3, and 5). However, unlike Kir2.1, Kir3.1/Kir3.4 is a heterotetramer and there is asymmetry at this position at the internal entrance to the selectivity filter. The data in Fig. 5 show that mutation of T-148 or A-172 in Kir3.4, but not A-142 or S-166 in Kir3.1, reduced Cs^+ block and enhanced Rb^+ permeation. This suggests that T-148 and A-172 in Kir3.4, and not the residues at the equivalent positions in Kir3.1, are critical in determining the characteristics of ion block and permeation of the Kir3.1/Kir3.4 channel. In Kir2.1, Thompson et al. (22) found no evidence that the two polar residues (T-141 and S-165) form a H^+ bond and neither do the data from this study support the presence of a H^+ bond between the equivalent residues in the Kir3.1/Kir3.4 channel. (In the Kir3.1/Kir3.4 channel, there could potentially only be a H^+ bond between Kir3.4-T-148 and Kir3.1-S-166 and the H^+ bond should be disrupted by the mutation of one or both of the residues to a nonpolar residue and the results in Figs. 5 and 6 do not support a scheme as simple as this.) In Kir2.1, Thompson et al. (22) instead suggested that T-141 and S-165 form binding sites for monovalent blocking cations. We suggest a different explanation below.

In the case of the Kir3.1/Kir3.4 channel, mutation of the equivalent residues affect spermine permeation, inward rectification, and agonist activation, as well as Cs^+ block and Rb^+ permeation (Figs. 5 and 10). We have previously shown that breaking the salt bridge between E-145 and R-155 behind the selectivity filter of Kir3.4 disrupts the selectivity filter—molecular dynamics modeling suggests that the salt bridge behind the selectivity filter is equivalent to the string of a bow and it tensions the selectivity filter and holds it in its correct configuration. As a result, when the salt bridge is disrupted, the selectivity filter becomes ''floppy''. The disruption of the salt bridge has dramatic effects on block, permeation, inward rectification, and agonist activation (9,16); the actions are similar to those (shown in this study) of mutating the residues at the base of the selectivity filter of Kir3.1/Kir3.4. For this reason, we suggest that the residues at the base of the selectivity filter do not themselves form binding sites for monovalent blocking cations (as suggested by Thompson et al. (22)). Instead we suggest that the residues at the base of the selectivity filter act in the same way as the salt bridge: in some way, they act to stabilize the selectivity filter in its normal configuration. Therefore, if the residues at the base of the selectivity filter are disturbed by mutation, the selectivity filter is disrupted in some way (once more, perhaps it becomes floppy) and as a result any property dependent on the selectivity filter (block and permeation and, possibly, inward rectification and agonist activation) is affected.

Interestingly, in the same way that only mutation of the residues at the base of the selectivity filter in Kir3.4 dramatically affects the channel (Fig. 5), only disruption of the salt bridge in Kir3.4 dramatically affects the channel (9). It is possible that these two facts are related: Figs. 8 and 9 show that, when the salt bridge in Kir3.1 was disrupted, dramatic and/or significant effects on channel properties were observed if simultaneously Kir3.1-A-142 was mutated to a threonine residue (resulting in TTTT at this position) or Kir3.4-T-148 was mutated to an alanine residue (resulting in AAAA at this position) (note that both of these mutations result in a symmetrical internal selectivity filter entrance). This interaction between the residues that form a salt bridge behind the selectivity filter and the residues at the base of the selectivity filter supports the hypothesis that mutation of either set of residues acts in the same way (i.e., by disrupting the selectivity filter).

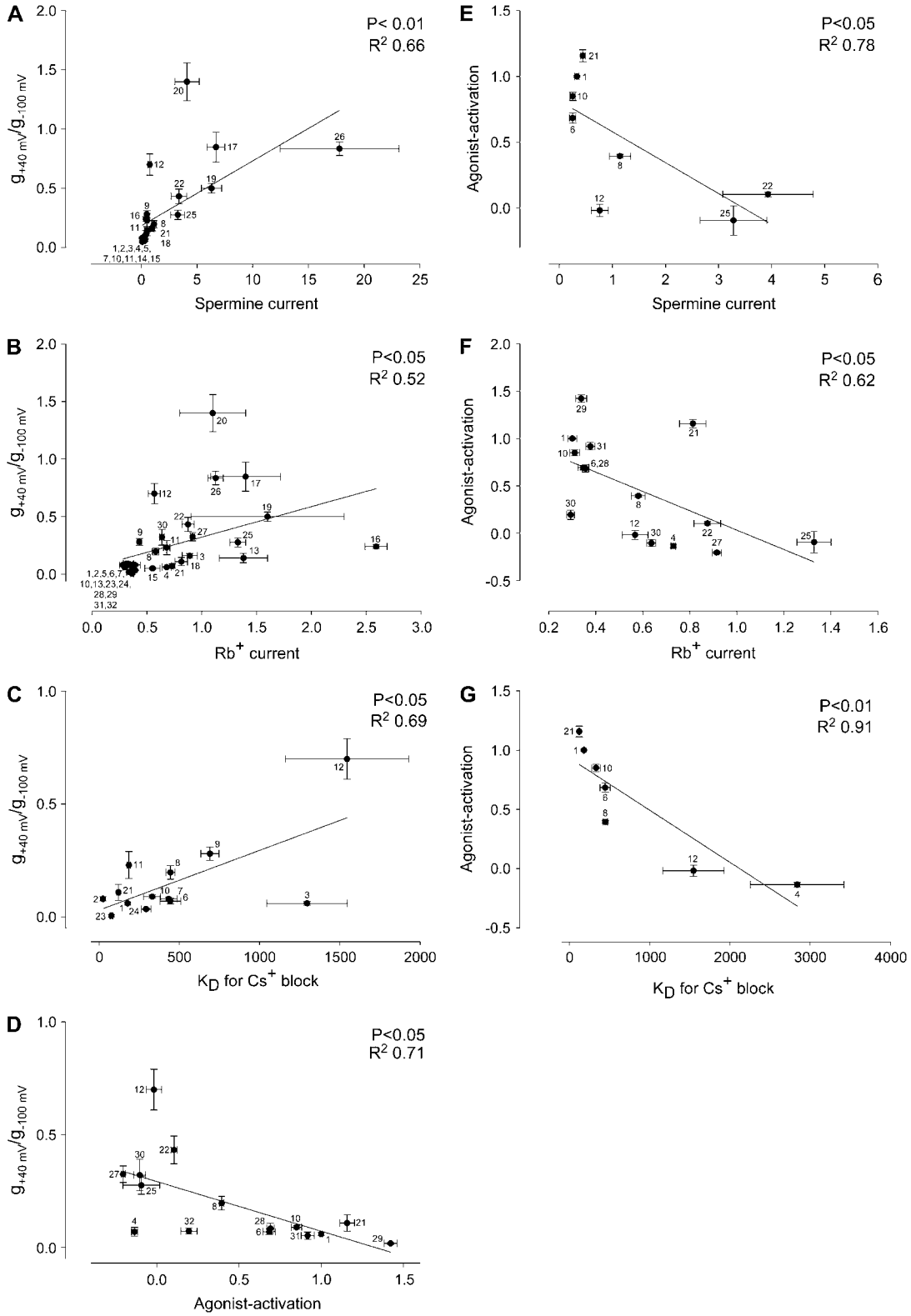

FIGURE 12 Correlations between Cs^+ block, Rb^+ and spermine permeation, inward rectification, and agonist activation. (*A–D*) Correlation between inward rectification ($g_{+40\ mV}/g_{-100\ mV}$) and spermine current (at −130 mV; *A*), Rb^+ current (at −130 mV; *B*), K_D (at −130 mV) of Cs^+ block (*C*) and agonist activation (*D*). Agonist activation was calculated as the fractional increase of current (at −130 mV) on application of agonist (agonist activation was 0 if there was no increase and 1 if current doubled on application of agonist). (*E–G*) Correlation between agonist activation and spermine current (at −130 mV; *E*), Rb^+ current (at −130 mV; *F*), and K_D (at −130 mV) of Cs^+ block (*G*). Data were fitted with a Pearson correlation (*P* and R^2 values shown). Wild-type and mutant

Inward rectification

In Kir2.1, mutation of residues in TM2 and the C-terminus (S-165, D-172, E-224, E-299) weaken inward rectification (2–6). Based on studies using different length amine molecules, Guo et al. (7,8) suggested that polyamines are stably coordinated within the intracellular pore by tethering the trailing end of the polyamine molecule at E-224 and E-299 and the leading head of the molecule at D-172. However, according to the alternative selectivity filter model (see Introduction), polyamines bind within the selectivity filter itself (9,10). Fig. 5 shows that inward rectification was weakened when Kir3.4-T-148, at the base of the selectivity filter, was mutated. Because Kir3.4-T-148 is at the base of the selectivity filter, it is closer to the selectivity filter than D-172 (its equivalent in the Kir3.1/Kir3.4 channel is Kir3.1-D-173) and as such should not affect inward rectification if the leading head of the polyamine molecule responsible for inward rectification is bound to D-172. As argued above, mutation of Kir3.4-T-148 disrupts the selectivity filter and, therefore, the loss of inward rectification on mutation of Kir3.4-T-148 in this study (Fig. 5) supports the selectivity filter model of inward rectification. The significant correlations between inward rectification and Cs^+ block and Rb^+ permeation in Fig. 12 also supports it (Cs^+ block and Rb^+ permeation are both properties of the selectivity filter).

Mutations that weakened inward rectification, such as replacement of Kir3.1-A-142 and Kir3.4-T-148 with valine residues (VVVV/**SASA**), also usually increased spermine permeability (Fig. 5). Indeed, the strength of inward rectification was significantly correlated with the ability of spermine to permeate the channel (Fig. 12 *A*). We have previously suggested that the permeability of Kir channels to polyamines ''fine-tunes'' the strength of inward rectification of the channels (11). The rationale behind this is that polyamines are permeant blockers of Kir channels and the more easily a polyamine molecule is able to permeate the channel (i.e., the selectivity filter), the less time it will spend blocking the channel. The significant correlation between inward rectification and spermine permeation in Fig. 12 *A* is consistent with this. However, this study has shown that there is not always a strict correlation between inward rectification and spermine permeation (e.g., Fig. 6 *A*). However, polyamine permeability of the selectivity filter is not expected to be the only factor controlling inward rectification. For example, a decrease in polyamine access to the selectivity filter is expected to decrease both inward rectification and spermine permeation.

Agonist activation

Binding of agonist to a G protein-coupled receptor releases $G_{\beta\gamma}$ and this interacts with the intracellular N- and C-termini of Kir3 channels to cause channel opening (31). The location of the gate that opens the channel after $G_{\beta\gamma}$ binding is unknown. Previous studies have shown that a number of mutations in TM2 also alter agonist activation of Kir3 channels (13–15). Based on their data, Jin et al. suggested that access of K^+ to the pore is gated at the ''bundle crossing'' by a pivoted bending motion of the TM2 helices about a highly conserved glycine residue (13). From a comparison of the crystal structures of KcsA (assumed to be closed) and Kv1.2 (assumed to be open) (32), for example, as well as spin labeling experiments (33), the bundle crossing is indeed thought to open during channel activation. Furthermore, access of Cd^{2+} (radius 73% of K^+) or Ag^+ (radius 95% of K^+), for example, to the inner vestibule in Kv channels (*Shaker* and HCN channels) is gated (34,35).

However, Fig. 10 shows that mutation of Kir3.1-A-142 and Kir3.4-T-148 to valine residues (VVVV/**SASA**) or of Kir3.1-S-166 and Kir3.4-A-172 to leucine residues (**ATAT**/LLLL) abolished agonist activation of the Kir3.1/Kir3.4 channel and this is consistent with our previous study that shows that disruption of the selectivity filter by disruption of the salt bridge behind the selectivity filter abolishes agonist activation (16). These data are not readily reconcilable with the possibility that the bundle crossing is the agonist-activated gate. One possibility is that the mutations at the selectivity filter allosterically affect the bundle crossing. However, this could not explain the correlation in Fig. 12 between agonist activation and selectivity (presumably dependent on the selectivity filter). The alternative possibility is that mutations in TM2 affect gating by allosterically affecting the selectivity filter. Consistent with this, mutation of the phenylalanine residues at the bundle crossing in Kir3.1/Kir3.4 affects selectivity as well as agonist activation (16).

Fig. 13 shows models of Kir3.1 (Fig. 13 *A*) and Kir3.4 (Fig. 13 *B*) subunits and an alignment of Kir3 channels (Fig. 13 *C*) with mutations reported to alter agonist activation highlighted. It is apparent in Fig. 13, *A* and *B*, that residues associated with agonist activation extend from the bundle

FIGURE 12 (Continued).

channels 1–21 were investigated in this study and mutant channels 22–35 were investigated in previous studies (9,16): 1 Kir3.1/Kir3.4 (wild-type); 2 Kir3.1-S-166L/Kir3.4; 3 Kir3.1/Kir3.4-A-172L; 4 Kir3.1-S-166L/Kir3.4-A-172L; 5 Kir3.1-S-166L-A-142T/Kir3.4; 6 Kir3.1-A-142T/Kir3.4; 7 Kir3.1-A-142V/Kir3.4; 8 Kir3.1/Kir3.4-T-148A; 9 Kir3.1/Kir3.4-T-148V; 10 Kir3.1-A-142T/Kir3.4-T-148A; 11 Kir3.1-A-142V/Kir3.4T-148-A; 12 Kir3.1-A-142V/Kir3.4-T-148V; 13 Kir3.1/Kir3.4-T-148A-A-172L; 14 Kir3.1-A-142T-S-166L/Kir3.4; 15 Kir3.1-A-142T-S-166L/Kir3.4-A-172L; 16 Kir3.1-S-166L/Kir3.4-T-148A-A-172L; 17 Kir3.1/Kir3.4-T-148A-E-145Q; 18 Kir3.1-A-142T-E-139Q/Kir3.4; 19 Kir3.1-A-142T/Kir3.4-T-148A-E-145Q; 20 Kir3.1-E-139Q/Kir3.4-T-148A; 21 Kir3.1-E-139Q/Kir3.4; 22 Kir3.1/Kir3.4-E-145Q; 23 Kir3.1-E-141Q/Kir3.4; 24 Kir3.1/Kir3.4-E-147Q; 25 Kir3.1/Kir3.4-R-155E; 26 Kir3.1-R-149E/Kir3.4-E-145Q; 27 Kir3.1/Kir3.4-E-145Q-R-155E; 28 Kir3.1-F-181M/Kir3.4; 29 Kir3.1/Kir3.4-F-187M; 30 Kir3.1-F-181A/Kir3.4-F-187A; 31. Kir3.1-F-181M/Kir3.4-F-187M; 32 Kir3.1-S-170P/Kir3.4-S-176P; 33 Kir3.1-D-173Q/Kir3.4; 34 Kir3.1/Kir3.4-E-231Q; and 35 Kir3.1-D-173Q/Kir3.4-E-231Q. Data corrected for junction potentials.

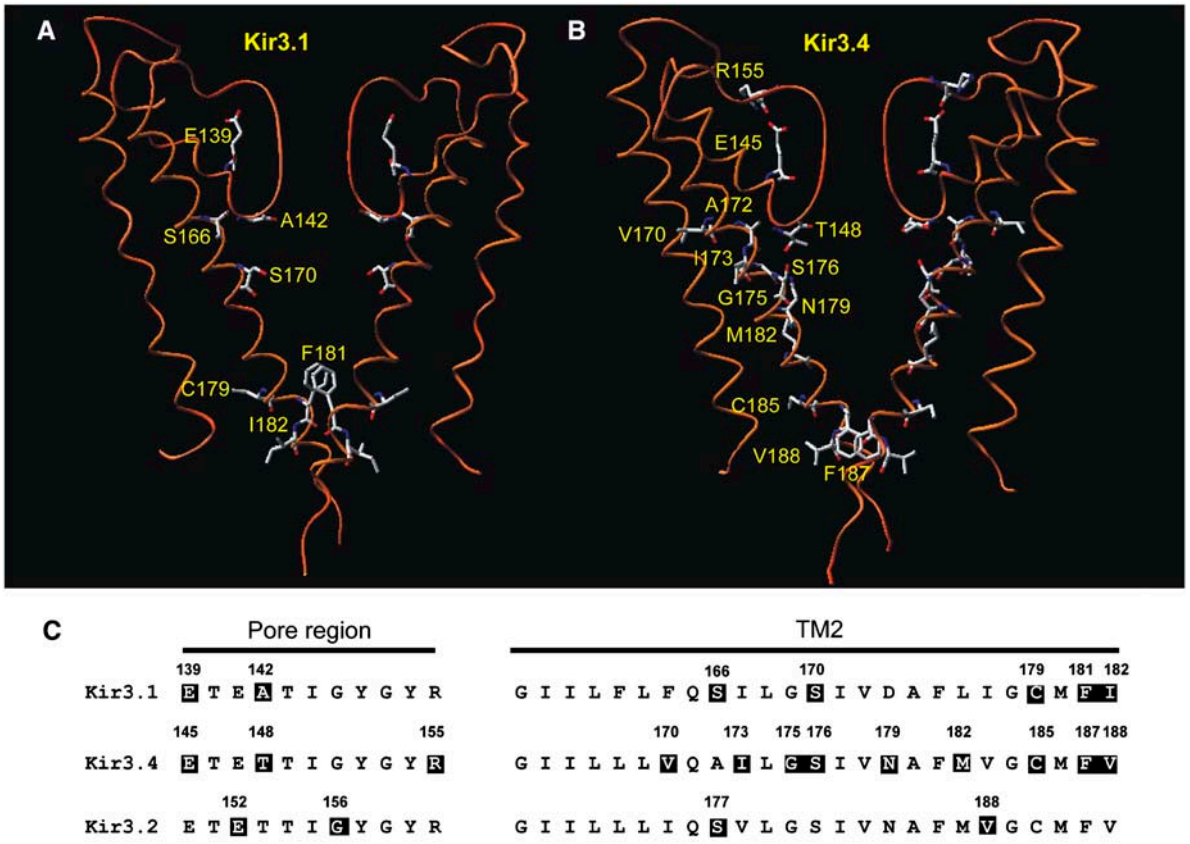

FIGURE 13 Summary of residues involved in agonist activation of Kir3 channels. (*A* and *B*) Models of the TM1-P-TM2 domains of the two Kir3.1 (*A*) or two Kir3.4 (*B*) subunits of the Kir3.1/Kir3.4 tetramer based on the KcsA crystal structure. Residues that when mutated abolish agonist activation are highlighted. (*C*) An alignment of the pore region (*left*) and TM2 domain (*right*) in Kir3.1, Kir3.4, and Kir3.2. Residues that when mutated abolish agonist activation are also highlighted. Kir3.1-E-139 (this study); Kir3.1-A-142 (this study); Kir3.1-S-166 (this study); Kir3.1-S-170 (14,16); Kir3.1-C-179 (14); Kir3.1-F-181 (16); Kir3.1-I-182 (14); Kir3.4-E-145 (16); Kir3.4-T-148 (this study); Kir3.4-R-155 (16); Kir3.4-V-170 (13); Kir3.4-I-173 (13); Kir3.4-G-175 (13); Kir3.4-S-176 (13,16); Kir3.4-N-179 (13); Kir3.4-M-182 (13); Kir3.4-C-185 (14); Kir3.4-F-187 (16); Kir3.4-V-188 (14); Kir3.2-E-152 (15); Kir3.2-G-156 (15); Kir3.2-S-177 (15); and Kir3.2-V-188 (15).

crossing, up the TM2 domains and across to the selectivity filter. Given this pattern of reactivity, we tentatively propose a working hypothesis for the mechanism of agonist activation of Kir3 channels. We suggest that binding of $G_{\beta\gamma}$ with the intracellular domain of the channel induces a pivoted bending of the TM2 domains about the conserved glycine at position 83 as suggested previously (13). However, we propose that this signal is then transduced along the TM2 domains up to the base of the selectivity filter, where small movements of the selectivity filter gate the access of K^+. This hypothesis is supported by the observation that the selectivity of Kir3.1/Kir3.4 changes during agonist activation (Fig. 11).

This hypothesis is also supported by other studies. In some channels at least, the bundle crossing may not be sufficient to impede the passage of permeant ions through the pore. Although access of large methanethiosulfonate (MTS) reagents (such as MTSET with radius ~218% of K^+) to the inner vestibule of a Ca^{2+}-activated K^+ channel (SK) and a cyclic nucleotide-gated channel (CNG1) is gated, smaller MTS reagents (such as MTSEA with radius ~135% of K^+) or Ag^+ (radius 95% of K^+) have state-independent access (36,37). Although access of MTSEA (radius ~135% of K^+) to the inner vestibule of Kir6.2 is gated (38), Ba^{2+}, which is more similar in size to K^+ (Ba^{2+} radius 102% of K^+), has state-independent access (17).

The concept of the selectivity filter as a gate is not novel: C-type inactivation in voltage-gated K^+ channels closes the channel by constriction of the outer mouth of the selectivity filter (39,40). In addition, the selectivity filter in Kir channels has been suggested to be responsible for ''fast gating'': Kir channels show bursting activity and mutations within the selectivity filter of Kir2.1 (41,42), Kir3.1/Kir3.4 (43), and Kir6.2 (44) or exchanging the P-loop of Kir2.1 with that of Kir1.1b (45) alter the activity within bursts, i.e., fast gating (short openings and closures).

In contrast to fast gating, ''slow gating'' (i.e., bursting characterized by the burst duration and interburst closed time) is affected by mutations close to the bundle crossing (44,46). Therefore, whereas fast gating may correspond to gating at the selectivity filter, slow gating may correspond to gating at the bundle crossing. Ivanova-Nikolova and Breitwieser (47)

showed that, in the native Kir3.1/Kir3.4 channel, fast gating (perhaps selectivity filter gating) is agonist dependent, whereas slow gating (perhaps bundle crossing gating) is agonist-independent. They showed that, as the agonist (ACh) concentration is increased, the number of openings per burst is increased, the open time is increased, and the closed time is reduced (47). This was subsequently confirmed by Nemec et al. (48). These findings are consistent with a significant role for the selectivity filter in agonist activation.

Other studies suggest that the selectivity filter may be coupled to gating: with the Weaver mutation, in which the second glycine residue in the GYG motif of the Kir3.2 G protein-activated channel is replaced by a serine residue, both selectivity and agonist activation are altered (49,50); the selectivity of cyclic nucleotide-gated channels for Ca^{2+} over Na^{+} increases with open probability (51); and the selectivity spectrum of a mutant *Shaker* channel changes as it passes through subconductance states on its way to the fully open state (52).

The possibility that the selectivity filter is altered during gating is supported by spin labeling experiments, which show that during channel activation there are small movements of the inner portion of the selectivity filter (at approximately the position of Kir3.1-A-142 and Kir3.4-T-148) (33). Again consistent with the possibility that the selectivity filter is a gate, evidence shows that the selectivity filter is flexible and not rigid: simulation studies of the dynamics of the KirBac1.1 channel show the occurrence of conformational distortions of the selectivity filter, especially in the absence of K^{+} (53), and it is clear that the selectivity filter of the KcsA channel is flexible given the different conformations adopted in the presence of different external K^{+} concentrations (54).

Is the selectivity filter responsible for both inward rectification and agonist activation?

In summary, we have observed that mutation of residues at the base of the selectivity filter alter both inward rectification and agonist activation. Unless the effects are allosteric, the data suggest that the selectivity filter is responsible for both agonist activation and inward rectification. Recently, Hommers et al. (26) showed that agonist activation of Kir3.1/Kir3.4 alters Ba^{2+} and Cs^{+} block and this confirms that the selectivity filter of Kir3.1/Kir3.4 is altered during agonist activation. Furthermore, Hommers et al. (26) showed that agonist activation alters inward rectification—in inside-out patches from rat atrial cells, we have also observed that the strength of inward rectification of Kir3.1/Kir3.4 depends on agonist activation (55). Hommers et al. (26) observed a significant correlation between Cs^{+} block and inward rectification similar to that in Fig. 12 *C* (although, in the experiments of Hommers et al. (26), the two were varied by agonist activation, whereas in Fig. 12 *C* the two were varied by mutatagenesis). These findings support the possibility that the selectivity filter may be responsible for both inward rectification and agonist activation. Indeed Hommers et al. (26) concluded that ''$G_{\beta\gamma}$ might gate the channel at the selectivity filter rather than at a cytoplasmic gate''. Similarly, Alagem et al. (43) in relation to Kir3.1/Kir3.4 concluded that ''the conformational changes at the TM2 induced by agonist binding at the intracellular side of the channel may only serve as a relay of signaling, to stabilize the opening of a physical gate located elsewhere in the channel''.

Nevertheless, in the case of the ATP-sensitive K^{+} channel, slow gating is ATP dependent (fast gating is ATP independent), and the mutation T-171A at the bundle crossing in Kir6.2 affects slow gating as well as ATP inhibition (56). Clearly, more direct physical measurements are needed to define the exact part of Kir channels that is controlling K^{+} flux.

REFERENCES

1. Lopatin, A. N., E. N. Makhina, and C. G. Nichols. 1994. Potassium channel block by cytoplasmic polyamines as the mechanism of intrinsic rectification. *Nature*. 372:366–369.
2. Stanfield, P. R., N. W. Davies, P. A. Shelton, M. J. Sutcliffe, I. A. Khan, W. J. Brammar, and E. C. Conley. 1994. A single aspartate residue is involved in both intrinsic gating and blockage by Mg^{+} of inward rectifier, IRK1. *J. Physiol.* 478:1–6.
3. Yang, J., Y. N. Jan, and L. Y. Jan. 1995. Control of rectification and permeation by residues in two distinct domains in an inward rectifier K^{+} channel. *Neuron*. 14:1047–1054.
4. Kubo, Y., and Y. Murata. 2001. Control of rectification and permeation by two distinct sites after the second transmembrane region in Kir2.1 K^{+} channel. *J. Physiol.* 531:645–660.
5. Lu, Z., and R. MacKinnon. 1994. Electrostatic tuning of Mg^{2+} affinity in an inward-rectifier K^{+} channel. *Nature*. 371:243–246.
6. Fujiwara, Y., and Y. Kubo. 2002. Ser165 in the second transmembrane region of the Kir2.1 channel determines its susceptibility to blockade by intracellular Mg^{2+}. *J. Gen. Physiol.* 120:677–693.
7. Guo, D., Y. Ramu, A. M. Klem, and Z. Lu. 2003. Mechanism of rectification in inward-rectifier K^{+} channels. *J. Gen. Physiol.* 121:261–275.
8. Guo, D., and Z. Lu. 2003. Interaction mechanisms between polyamines and IRK1 inward rectifier K^{+} channels. *J. Gen. Physiol.* 122:485–500.
9. Dibb, K. M., T. Rose, S. Y. Makary, T. W. Claydon, D. Enkvetchakul, R. Leach, C. G. Nichols, and M. R. Boyett. 2003. Molecular basis of ion selectivity, block, and rectification of the inward rectifier Kir3.1/Kir3.4 K^{+} channel. *J. Biol. Chem.* 278:49537–49548.
10. Kurata, H. T., L. R. Phillips, T. Rose, G. Loussouarn, S. Herlitze, H. Fritzenschaft, D. Enkvetchakul, C. G. Nichols, and T. Baukrowitz. 2004. Molecular basis of inward rectification: polyamine interaction sites located by combined channel and ligand mutagenesis. *J. Gen. Physiol.* 124:541–554.
11. Makary, S. M., T. W. Claydon, D. Enkvetchakul, C. G. Nichols, and M. R. Boyett. 2005. A difference in inward rectification and polyamine block and permeation between the Kir2.1 and Kir3.1/Kir3.4 K^{+} channels. *J. Physiol.* 568:749–766.
12. Xie, L. H., S. A. John, and J. N. Weiss. 2003. Inward rectification by polyamines in mouse Kir2.1 channels: synergy between blocking components. *J. Physiol.* 550:67–82.
13. Jin, T., L. Peng, T. Mirshahi, T. Rohacs, K. W. Chan, R. Sanchez, and D. E. Logothetis. 2002. The $\beta\gamma$ subunits of G proteins gate a K^{+} channel by pivoted bending of a transmembrane segment. *Mol. Cell.* 10:469–481.
14. Sadja, R., K. Smadja, N. Alagem, and E. Reuveny. 2001. Coupling $G\beta\gamma$-dependent activation to channel opening via pore elements in inwardly rectifying potassium channels. *Neuron*. 29:669–680.

15. Yi, B. A., Y. F. Lin, Y. N. Jan, and L. Y. Jan. 2001. Yeast screen for constitutively active mutant G protein-activated potassium channels. *Neuron*. 29:657–667.

16. Claydon, T. W., S. Y. Makary, K. M. Dibb, and M. R. Boyett. 2003. The selectivity filter may act as the agonist-activated gate in the G protein-activated Kir3.1/Kir3.4 K^+ channel. *J. Biol. Chem.* 278:50654–50663.

17. Proks, P., J. F. Antcliff, and F. M. Ashcroft. 2003. The ligand-sensitive gate of a potassium channel lies close to the selectivity filter. *EMBO Rep*. 4:70–75.

18. Xiao, J., X. G. Zhen, and J. Yang. 2003. Localization of PIP2 activation gate in inward rectifier K^+ channels. *Nat. Neurosci.* 6:811–818.

19. Lancaster, M. K., K. M. Dibb, C. Quinn, R. Leach, J.-K. Lee, J. B. C. Findlay, and M. R. Boyett. 2000. Residues and mechanisms for slow activation and Ba^{2+} block of the cardiac muscarinic K^+ channel, Kir3.1/Kir3.4. *J. Biol. Chem.* 275:35831–35839.

20. Doyle, D. A., J. M. Cabral, R. A. Pfuetzner, A. Kuo, J. M. Gulbis, S. L. Cohen, B. T. Chait, and R. MacKinnon. 1998. The structure of the potassium channel: molecular basis of K^+ conduction and selectivity. *Science*. 280:69–77.

21. Yang, J., M. Yu, Y. N. Jan, and L. Y. Jan. 1997. Stabilization of ion selectivity filter by pore loop ion pairs in an inwardly rectifying potassium channel. *Proc. Natl. Acad. Sci. USA*. 94:1568–1572.

22. Thompson, G. A., M. L. Leyland, I. Ashmole, M. J. Sutcliffe, and P. R. Stanfield. 2000. Residues beyond the selectivity filter of the K^+ channel Kir2.1 regulate permeation and block by external Rb^+ and Cs^+. *J. Physiol.* 526:231–240.

23. Silverman, S. K., H. A. Lester, and D. A. Dougherty. 1998. Asymmetrical contributions of subunit pore regions to ion selectivity in an inward rectifier K^+ channel. *Biophys. J.* 75:1330–1339.

24. Slesinger, P. A. 2001. Ion selectivity filter regulates local anesthetic inhibition of G-protein-gated inwardly rectifying K^+ channels. *Biophys. J.* 80:707–718.

25. Hidalgo, P., and R. MacKinnon. 1995. Revealing the architecture of a K^+ channel pore through mutant cycles with a peptide inhibitor. *Science*. 268:307–310.

26. Hommers, L. G., M. J. Lohse, and M. Bunemann. 2003. Regulation of the inward rectifying properties of G-protein-activated inwardly rectifying K^+ (GIRK) channels by $G\beta\gamma$ subunits. *J. Biol. Chem.* 278: 1037–1043.

27. Berneche, S., and B. Roux. 2004. A gate in the selectivity filter of potassium channels. *Biophys. J.* 86:9a. (Abstr.)

28. Peleg, S., D. Varon, T. Ivanina, C. W. Dessauer, and N. Dascal. 2002. $G\alpha_i$ controls the gating of the G protein-activated K^+ channel, GIRK. *Neuron*. 33:87–99.

29. Claydon, T. W., S. Y. Makary, and M. R. Boyett. 2002. A difference in polyamine permeation of the Kir2.1 and Kir3.1/Kir3.4 inwardly-rectifying K^+ channels underlies a difference in inward rectification. *J. Physiol.* 544:11P. (Abstr.)

30. Makary, S. Y., T. W. Claydon, and M. R. Boyett. 2003. The weaker inward rectification of Kir3.1/Kir3.4 compared to that of Kir2.1 may be the result of a higher polyamine permeability. *Biophys. J.* 84:314a. (Abstr.)

31. Finley, M., C. Arrabit, C. Fowler, K. F. Suen, and P. A. Slesinger. 2004. βL-βM loop in the C-terminal domain of G protein-activated inwardly rectifying K^+ channels is important for $G_{\beta\gamma}$ subunit activation. *J. Physiol.* 555:643–657.

32. Long, S. B., E. B. Campbell, and R. MacKinnon. 2005. Crystal structure of a mammalian voltage-dependent Shaker family K^+ channel. *Science*. 309:897–903.

33. Perozo, E., D. M. Cortes, and L. G. Cuello. 1999. Structural rearrangements underlying K^+-channel activation gating. *Science*. 285: 73–78.

34. del Camino, D., and G. Yellen. 2001. Tight steric closure at the intracellular activation gate of a voltage-gated K^+ channel. *Neuron*. 32:649–656.

35. Rothberg, B. S., K. S. Shin, P. S. Phale, and G. Yellen. 2002. Voltage-controlled gating at the intracellular entrance to a hyperpolarization-activated cation channel. *J. Gen. Physiol.* 119:83–91.

36. Flynn, G. E., and W. N. Zagotta. 2001. Conformational changes in S6 coupled to the opening of cyclic nucleotide-gated channels. *Neuron*. 30:689–698.

37. Bruening-Wright, A., M. A. Schumacher, J. P. Adelman, and J. Maylie. 2002. Localization of the activation gate for small conductance Ca^{2+}-activated K^+ channels. *J. Neurosci.* 22:6499–6506.

38. Phillips, L. R., D. Enkvetchakul, and C. G. Nichols. 2003. Gating dependence of inner pore access in inward rectifier K^+ channels. *Neuron*. 37:953–962.

39. Kiss, L., J. LoTurco, and S. J. Korn. 1999. Contribution of the selectivity filter to inactivation in potassium channels. *Biophys. J.* 76:253–263.

40. Rasmusson, R. L., M. J. Morales, S. Wang, S. Liu, D. L. Campbell, M. V. Brahmajothi, and H. C. Strauss. 1998. Inactivation of voltage-gated cardiac K^+ channels. *Circ. Res.* 82:739–750.

41. Guo, L., and Y. Kubo. 1998. Comparison of the open-close kinetics of the cloned inward rectifier K^+ channel IRK1 and its point mutant (Q140E) in the pore region. *Receptors Channels*. 5:273–289.

42. Lu, T., A. Y. Ting, J. Mainland, L. Y. Jan, P. G. Schultz, and J. Yang. 2001. Probing ion permeation and gating in a K^+ channel with back bone mutations in the selectivity filter. *Nat. Neurosci.* 4:239–246.

43. Alagem, N., S. Yesylevskyy, and E. Reuveny. 2003. The pore helix is involved in stabilizing the open state of inwardly rectifying K^+ channels. *Biophys. J.* 85:300–312.

44. Proks, P., C. E. Capener, P. Jones, and F. M. Ashcroft. 2001. Mutations within the P-loop of Kir6.2 modulate the intraburst kinetics of the ATP-sensitive potassium channel. *J. Gen. Physiol.* 118:341–353.

45. Choe, H., L. G. Palmer, and H. Sackin. 1999. Structural determinants of gating in inward-rectifier K^+ channels. *Biophys. J.* 76:1988–2003.

46. Trapp, S., P. Proks, S. J. Tucker, and F. M. Ashcroft. 1998. Molecular analysis of ATP-sensitive K channel gating and implications for channel inhibition by ATP. *J. Gen. Physiol.* 112:333–349.

47. Ivanova-Nikolova, T. T., and G. E. Breitwieser. 1997. Effector contributions to $G\beta\gamma$-mediated signaling as revealed by muscarinic potassium channel gating. *J. Gen. Physiol.* 109:245–253.

48. Nemec, J., K. Wickman, and D. E. Clapham. 1999. $G\beta\gamma$ binding increases the open time of I_{KACh}: kinetic evidence for multiple $G\beta\gamma$ binding sites. *Biophys. J.* 76:246–252.

49. Kofuji, P., M. Hofer, K. J. Millen, J. H. Millonig, N. Davidson, H. A. Lester, and M. E. Hatten. 1996. Functional analysis of the weaver mutant GIRK2 K^+ channel and rescue of weaver granule cells. *Neuron*. 16:941–952.

50. Slesinger, P. A., N. Patil, Y. J. Liao, Y. N. Jan, L. Y. Jan, and D. R. Cox. 1996. Functional effects of the mouse weaver mutation on G protein-gated inwardly rectifying K^+ channels. *Neuron*. 16:321–331.

51. Hackos, D. H., and J. I. Korenbrot. 1999. Divalent cation selectivity is a function of gating in native and recombinant cyclic nucleotide-gated ion channels from retinal photoreceptors. *J. Gen. Physiol.* 113:799–818.

52. Zheng, J., and F. J. Sigworth. 1997. Selectivity changes during activation of mutant Shaker potassium channels. *J. Gen. Physiol.* 110: 101–117.

53. Domene, C., A. Grottesi, and M. S. Sansom. 2004. Filter flexibility and distortion in a bacterial inward rectifier K^+ channel: simulation studies of KirBac1.1. *Biophys. J.* 87:256–267.

54. Morais-Cabral, J. H., Y. Zhou, and R. MacKinnon. 2001. Energetic optimization of ion conduction rate by the K^+ selectivity filter. *Nature*. 414:37–42.

55. Shui, Z., and M. R. Boyett. 2004. Agonist-dependent inward rectification of the muscarinic K^+ channel in rat atrial cells. *Biophys. J.* 86:440a. (Abstr.)

56. Drain, P., X. Geng, and L. Li. 2004. Concerted gating mechanism underlying K_{ATP} channel inhibition by ATP. *Biophys. J.* 86:2101–2112.